Aerosol and Air Quality Research, 15: 2094–2103, 2015

ISSN: 1680-8584 print / 2071-1409 online
doi: 10.4209/aaqr.2015.03.0176

Simultaneous Control of Elemental Mercury/Sulfur Dioxide/Nitrogen Monoxide from Coal-Fired Flue Gases with Metal Oxide-Impregnated Activated Carbon

Chun-Hsiang Chiu[1], Hong-Ping Lin[2], Tien-Ho Kuo[3], Shiao-Shing Chen[1], Tien-Chin Chang[1], Kai-Han Su[1], Hsing-Cheng Hsi[4*]

[1] *Institute of Environmental Engineering and Management, National Taipei University of Technology, No. 1, Sec. 3, Chung-Hsiao E. Rd., Taipei 106, Taiwan*
[2] *Department of Chemistry, National Cheng-Kung University, No.1, University Rd., Tainan 701, Taiwan*
[3] *Department of Environmental Engineering, Tungnan University, No. 152, Sec. 3, Peishen Rd., Shenkeng District, New Taipei City 222, Taiwan*
[4] *Graduate Institute of Environmental Engineering, National Taiwan University, No. 71, Chou-Shan Rd., Taipei 106, Taiwan*

ABSTRACT

This research investigated the effects of transition metal oxide impregnation on the physical/chemical properties and on the multipollutant (i.e., $Hg^0/SO_2/NO$) control of a commercial coconut shell-based activated carbon. V, Mn, and Cu oxides of 5 wt% as their precursor metal hydroxides were impregnated onto the activated carbon surface. After the transition metal oxide impregnation, the surface area and pore volume of activated carbon decreased. The surface morphology of activated carbons was similar prior to and after impregnation. Mn^{3+}/Mn^{4+} and Cu^{+}/Cu^{2+} were shown to be the major valence states presenting in the MnO_x and CuO_x/CAC samples, respectively. CuO_x/CAC possessed the greatest Hg^0 removal efficiency of approximately 54.5% under N_2 condition and 98.9% under flue gas condition, respectively at 150°C. When the gas temperature increased to 350°C, the metal oxide-impregnated activated carbon still possessed appreciable Hg^0 removal, especially for CuO_x/CAC. The VO_x/CAC had the largest SO_2 removal enhancement of approximately 28.3% at 350°C. The NO removal of raw and impregnated activated carbon was very small under flue gas condition, indicating that adsorption of NO using metal oxide-impregnated activated carbon may not be a suitable route for NO control.

Keywords: Elemental mercury; Multipollutant control; Metal oxide; Activated carbon; Coal combustion.

INTRODUCTION

Mercury (Hg) is a global pollutant, highly harmful to human, animals, and plants. Coal combustion has been known as one of the major anthropogenic sources of atmospheric Hg, contributing 30% of the total anthropogenic Hg emission (Pacyna *et al*., 2010). Hg emission from coal-fired power plants (CFPPs) has aroused the greatest concern to the public due to its unique physicochemical properties, high toxicity, long retention time in the environment, and potentially adverse effects on the ecosystem. The Minamata Convention on Mercury delivered in March 19, 2013 addressed the necessity of prevention and abatement of Hg emission and release via global and legally-binding agreements between countries (UNEP, 2013). Consequently, several countries have implemented or is proposing more stringent regulations on the abatement of Hg emissions. In October 2013, Taiwan Environmental Protection Administration has promulgated a new regulation for limiting Hg emissions from coal-fired steam and cogeneration boilers; the Hg emission should be lowered than 2 and 5 $\mu g\,Nm^{-3}$ for new and existing facilities, respectively (Taiwan Environmental Protection Administration, 2013).

The three stable forms of Hg in the coal-fired flue gas: elemental (Hg^0), oxidized (Hg^{2+}) and particulate-bound (Hg_p) govern the fate of this species (Yan *et al*., 2005; Granite *et al*., 2006; Li *et al*., 2012). The Hg^{2+} and Hg_p can be successfully removed with the existing air pollution control devices (APCD) in CFPPs. Hg^{2+} can be easily removed by wet flue gas desulfurization because Hg^{2+} is highly soluble in water. Hg_P can be captured by fly ash by particulate control systems (e.g., electrostatic precipitators, fabric filters, or baghouses) (Li *et al*., 2012). Nevertheless, low-level Hg^0 in CFPP flue gases is very difficult to remove

* Corresponding author.
Tel.: +886 2 33664374; Fax: +886 2 23928830
E-mail address: hchsi@ntu.edu.tw

with conventional APCD because Hg^0 is highly volatile and nearly insoluble in water.

Activated carbon has been considered excellent adsorbent for Hg control (Granite *et al.*, 2006; Hsi and Chen, 2012; Hsi *et al.*, 2013). Some studies have reported the individual and simultaneous removal of Hg, SO_2, and NO under flue gas conditions by carbon-based materials (e.g., activated carbon, activated coke, and activated carbon fibers) (Stencel and Rubel, 1995; Tsuji and Shiraishi, 1997; Mochida *et al*., 1999). Karatza *et al*. (2000) reported that S, Cl, I-impregnated activated carbon exhibited great potential for Hg^0 removal under flue gas condition. Hu *et al*. (2014) showed that activated carbon (AC-CS, made from coconut shell) can be used to remove Hg^0 and the process was complete chemisorption in simulated flue gas. One study also indicated that incorporation of sulfur groups on the activated carbon can enhance the oxidation of Hg^0 into Hg^{2+} and subsequently bonded with oxidized Hg, resulting in higher Hg capacities (Yao *et al*., 2014).

Besides sulfur and halogen surface functionality, metal oxides have been shown to greatly increase the Hg^0 adsorption or oxidation performance of activated carbon. Mei *et al*. (2008) indicated that high loading values and adsorption temperatures increased the Hg^0 removal percentage by Co_3O_4-doped activated carbon; the $CuCoO_4$-doped activated carbon also showed the greatest SO_2 removal efficiency. Tian *et al*. (2009) demonstrated that the doped CeO_2 in activated carbon significantly promoted the adsorption ability for Hg^0. Sumathi *et al.* (2010) indicated that the raw and the palm shell-based activated carbons impregnated with Ni, V, Fe and Ce metal oxides can be used to simultaneous removal of SO_2 and NO_x. Liu and Liu (2013) suggested that activated coke doped with V metal oxide had high activities in adsorption and oxidation, which are the key mechanisms for multipollutants removal in coal-fired flue gas. Du *et al*. (2014) indicated that $CuCl_2$-impregnated activated carbon had higher adsorption ability for Hg^0 as compared to those for $CuCl_2$-impregnated neutral Al_2O_3 and zeolite at 60–300°C.

The findings in the aforementioned literatures lead to a conclusion that metal-oxide doped or impregnated activated carbons could be highly feasible in control of Hg^0 via adsorption or oxidation effectively. Nevertheless, better comprehension on the effectiveness of multipollutant (i.e., Hg^0, SO_2, and NO) control using activated carbon modified with transition metal oxides is still limited and critical. The present research investigated the effects of transition metal oxide impregnation, including V, Mn, and Cu oxides, on the physiochemical properties and simultaneous $Hg^0/SO_2/NO$ control using a coconut shell-based activated carbon. A simulated coal-combustion flue gas generation platform associated a Hg^0/flue gas component monitoring system was used for the simultaneous Hg^0, SO_2, and NO removal experiments. The obtained results are important not only in the manner of Hg^0 emission control, but also on reducing the emissions of SO_2 and NO, which have been recognized as significant precursors of $PM_{2.5}$ that has cause markedly adverse effects in Asian countries.

MATERIALS AND METHODS

Preparation and Characterization of Metal Oxide-Impregnated Activated Carbon

A commercial coconut shell-based activated carbon (G-135; designated CAC in this paper) was obtained from China Activated Carbon Industries Ltd., Taiwan. To prepare the V, Mn, and Cu oxide-impregnated activated carbons, their corresponding metal hydroxides were precipitated to the activated carbon via a hydrothermal sol-gel method at a weight percentage of 5 wt% (as the precursor) followed with calcination (Chiu *et al*., 2014a). Metal salts including $V(OH)_5$, $Mn(OH)_2$, and $Cu(OH)_2$ were individually dissolved in water at a metal salt to water mass ratio of 0.04 wt%. The metal salt solution was then neutralized with 1.0 M NaOH aqueous solution to form precipitate at a proper pH value (i.e., $V(OH)_5$ precipitates at pH ≈5.0; $Mn(OH)_2$ precipitates at pH ≈10.0; $Cu(OH)_2$ precipitates at pH ≈11.0). After the precipitation process, powdered activated carbon with a precursor metal oxide to activated carbon mass ratio = 5.0 wt% was added to the metal hydroxide gel solution and further stirred for 2–3 h. The mixture was then transferred to an autoclave and statically heated at 100°C for 1 d. Filtration, washing, and drying gave the transition metal oxide-impregnated activated carbon products. The resulting metal oxide-impregnated activated carbons were ground into powder, passed through 200-mesh sieve, and stored for subsequent sample characterization and $Hg^0/SO_2/NO$ removal tests.

Detailed descriptions regarding physical characterization of samples can be found elsewhere (Chiu *et al*., 2014a). Briefly, the total surface area (S_{BET}), total pore volume (V_t), micropore (pore width < 2 nm) surface area (S_{micro}), and micropore volume (V_{micro}) of raw and metal oxide-impregnated activated carbon were determined based on N_2 adsorption obtained at 77 K (Quantachrome NOVA 2000e). The surface morphology was characterized using a scanning electron microscope (SEM; Hitachi S-4800). The crystal phase was examined with an X-ray diffractometer (XRD; PANalytical X'Pert PRO). X-ray photoelectron spectroscopy (XPS; Physical Electronics ESCA PHI 1600) analysis was used to understand the surface chemical compositions and the valance state of metal oxides on the activated carbon surface.

Multipollutant ($Hg^0/SO_2/NO$) Control Tests

Hg^0 removal tests were carried out at 150 and 350°C, respectively, in a fixed-bed testing apparatus using N_2 or a simulated coal-combustion flue gas as the carrier gas containing 27 ± 5 μg Nm^{-3} Hg^0 (Fig. 1; Chiu *et al*., 2014a, b). The reason to conduct the tests at these two temperatures was to evaluate the feasibility of applying the activated carbon directly at the outlet of a $DeNO_x$ catalyst or at the inlet of a hot-side electrostatic precipitator (both with a temperature ≈350°C) and at the inlet of a cold-side electrostatic precipitator (with a temperature ≈ 150°C). In the testing apparatus, Hg^0 was generated with a certificated Hg^0 permeation tube (VICI Metronics) in a gas generator at 70 ± 0.1°C to ensure a constant Hg^0 diffusion rate. The simulated

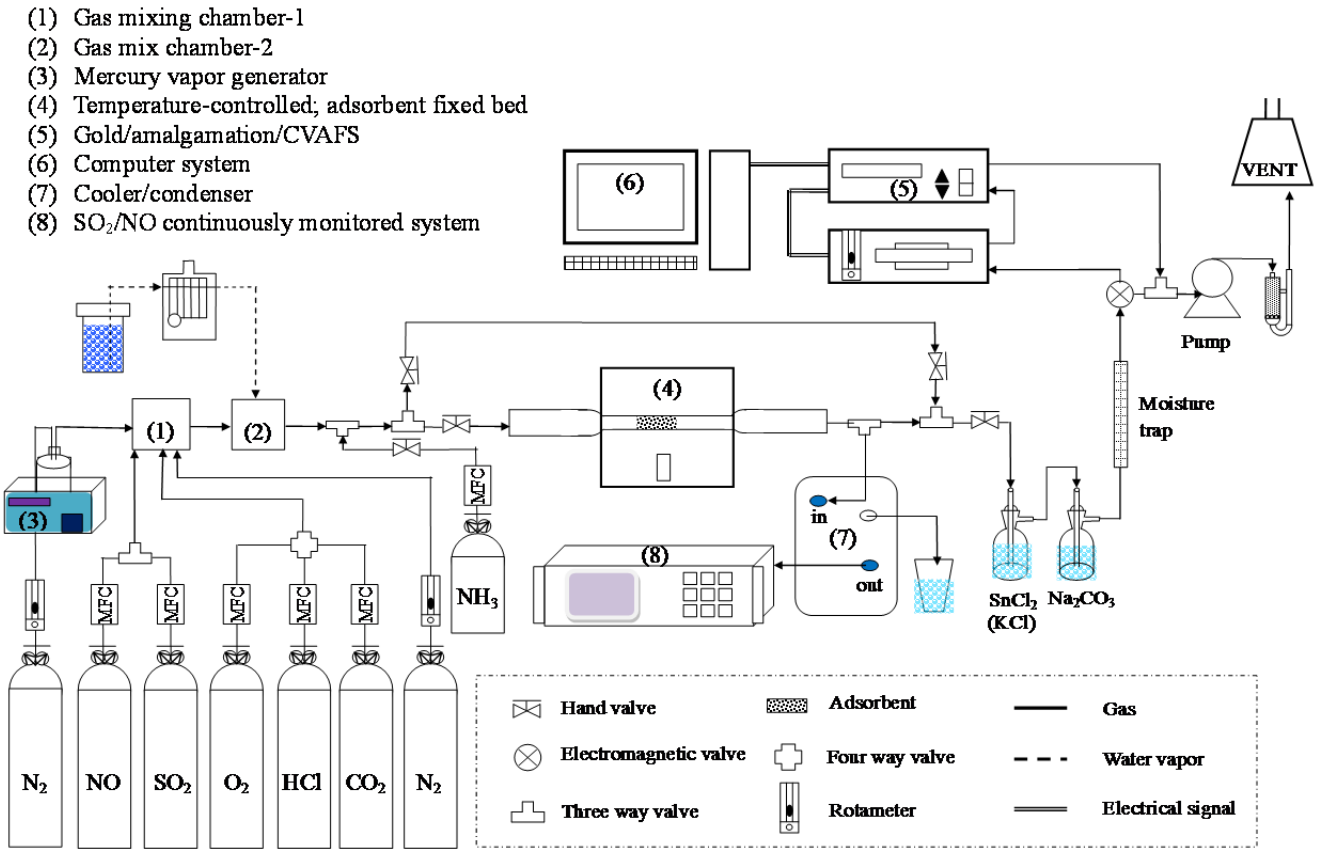

Fig. 1. Experimental system for fixed-bed multipollutant removal tests using raw and metal oxide-impregnated activated carbons (Chiu *et al*., 2014a, b).

flue gas also contained 14 vol% CO_2, 10 vol% H_2O, 6 vol% O_2, 50 ppm_v HCl, 200 ppm_v SO_2, 200 ppm_v NO, and balanced N_2 prepared from standard gas cylinders (Hsi and Chen, 2012). The composition of the flue gas was chosen to simulate the typical condition of coal-fired power plants in Taiwan, where low-sulfur bituminous and subbituminous coal blends are typically fired. The resulting gas stream passed through a temperature- controlled fixed-bed column (0.5-in i.d.) containing a 10 mg sample mixed with 0.5 g sand. The gas flow through an empty column was about 1.5 L min^{-1} at 25°C. The column length of the sample/sand mixture was about 1.5 cm and the time for gas stream to pass the mixture was approximately 0.3 s. The effluent gas from the fixed-bed column flowed through heated lines to an impinger containing $SnCl_{2(aq)}$ that reduced any oxidized Hg compounds to Hg^0. Gas exiting the impinger solutions flowed through a gold amalgamation column housed in a tubular furnace where the Hg in the gas was adsorbed. The Hg concentrated on the gold was then thermally desorbed and sent as a concentrated Hg stream to a cold-vapor atomic fluorescence spectrophotometer (CVAFS; Brooks Rand Lab Model III) for analysis. The experiment was performed for 900 min, or ceased until 100% breakthrough achieved. The Hg^0 removal performance was then calculated based on the breakthrough results obtained from the CVAFS measurements. The average Hg^0 removal can be subsequently calculated by the following equation:

$$\text{Average } Hg^0 \text{ removal percentage} = \frac{1}{n}\sum\frac{\left[CHg_{in}^{0} - CHg_{out}^{0}\right]}{CHg_{in}^{0}} \times 100\% \quad (1)$$

where CHg_{in}^{0} is the concentration of inlet Hg^0 (μg Nm^{-3}) and CHg_{out}^{0} is the concentration of outlet Hg^0 (μg Nm^{-3}). The total test number n is 150 because 6 min was required to obtain one data point within the 900 min experiment.

The outlet SO_2 and NO levels were continuously monitored with a flue gas component analyzer (Sick Maihak S710). The experiment was carried out simultaneously with the Hg^0 removal experiment for 900 min. Because a portion of the downstream SO_2 and NO was captured by the cooler/ condenser located prior to the flue gas analyzer due to the presence of H_2O, the SO_2 and NO removal enhancement was calculated respectively by:

$$SO_2 \text{ removal enhancement } (\eta_{SO_2};\ \%) = \frac{\left[C_{SO_2}^{blank} - C_{SO_2}^{out}\right]}{C_{SO_2}^{blank}} \times 100\% \quad (2)$$

$$\text{NO conversion enhancement } (\eta_{NO};\ \%) = \frac{\left[C_{NO}^{blank} - C_{NO}^{out}\right]}{C_{NO}^{blank}} \times 100\% \quad (3)$$

where $C_{SO_2}^{blank}$ and C_{NO}^{blank} indicate SO_2 and NO concentrations obtained from blank tests, respectively. The blank tests were performed under the simulated flue gas condition and without the presence of activated carbon samples. $C_{So_2}^{out}$ and C_{NO}^{out} are the SO_2 and NO concentrations in the outlet stream, respectively, when activated carbon particles are in the fixed-bed reactor.

RESULTS AND DISCUSSION

Physical and Chemical Characterization of Raw and Metal Oxide-Impregnated Activated Carbon

Table 1 shows the physical properties of raw and transition metal oxide-impregnated activated carbons. Raw CAC had S_{BET} of approximately 1230 $m^2\ g^{-1}$ and micropore S_{micro} of 1108 $m^2\ g^{-1}$ (i.e., 90% microporosity based on S_{micro}/S_{BET}). The S_{BET} and S_{micro} of treated CAC reduced to within 1085–1223 $m^2\ g^{-1}$ and 971.8–1089 $m^2\ g^{-1}$, respectively, corresponding to 89–92% microporosity. The CuO_x/CAC sample had the smaller S_{BET} and S_{micro} of 1090 and 971.8 $m^2\ g^{-1}$, respectively. Based on the obtained results, the decrease in surface area and pore volume of activated carbon was due to the pore blockage or filling by the impregnated transition metal oxides. These physical property analyses also verify that the raw and metal oxide-impregnated CACs can be classified as microstructural adsorbents.

Changes in surface morphology for activated carbons were observed after metal oxide impregnation (Fig. 2). Nevertheless, the surface morphology change, except for MnO_x/CAC, was not significant, suggesting a fairly uniform distribution of metal oxides in activated carbon samples.

Surface compositions of the activated carbons based on XPS analysis are shown in Table 2. The analytical results showed the presence and relative contents of carbon and oxygen in the raw activated carbon. After metal oxide impregnation, the amounts of impregnated transition metals (Mn and Cu) and oxygen increased and carbon content decreased accordingly. For MnO_x/CAC, deconvolution resulted in two fitting peaks corresponding to 641.0 and 642.3 eV, which can be assigned to the oxidation state of Mn^{3+} and Mn^{4+}, respectively. The data are encouraging because an increasing ratio of Mn^{4+}/Mn^{3+} could promote the Hg^0 oxidation (Ji *et al*., 2008; Li *et al*., 2010; Tian *et al*., 2011; Li *et al*., 2012). For the XPS result of CuO_x/CAC, two peaks corresponding to 931.8 and 934.1 eV can be deconvoluted and assigned to the oxidation state of Cu^+ and Cu^{2+}, respectively. An earlier study also confirmed that main peaks of Cu $2p_{3/2}$ were from 926 to 939 eV and Cu^+ and

Table 1. Physical properties of raw and transition metal oxide-impregnated activated carbons.

Sample[a]	S_{BET} ($m^2\ g^{-1}$)	S_{micro} ($m^2\ g^{-1}$)	S_{micro}/S_{BET} (%)	V_t ($cm^3\ g^{-1}$)	V_{micro} ($cm^3\ g^{-1}$)	V_{micro}/V_t (%)
Raw CAC	1230	1108	90	0.69	0.59	86
VO_x/CAC	1223	1089	89	0.69	0.57	83
MnO_x/CAC	1085	1003	92	0.61	0.53	87
CuO_x/CAC	1090	971.8	89	0.61	0.51	84

[a] S_{BET}: total surface area; S_{micro}: micropore area; V_t: total pore volume; V_{micro}: micropore volume.

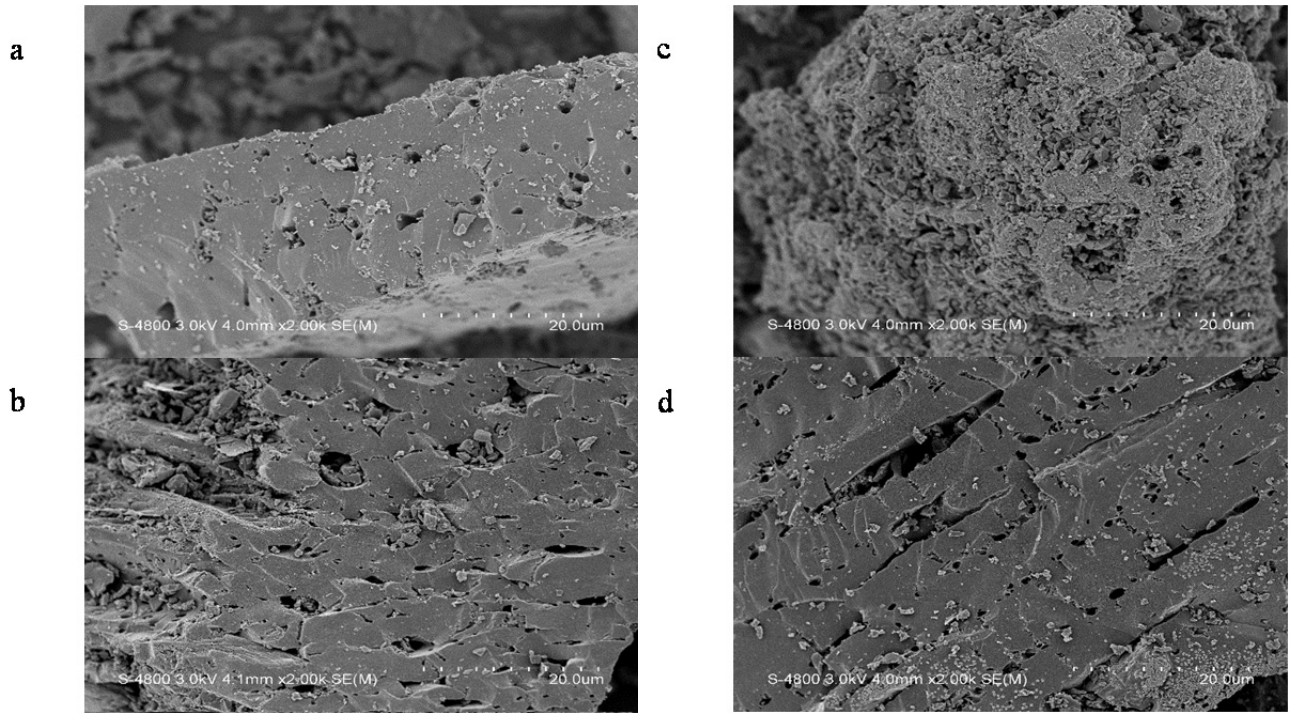

Fig. 2. SEM images of the activated carbons: (a) raw sample; (b) VO_x/CAC; (c) MnO_x/CAC; (d) CuO_x/CAC.

Table 2. Surface compositions of raw and transition metal oxide-impregnated activated carbons based on XPS results.

Sample	Atomic concentration of elements by XPS (at %)				
	C_{1s}	O_{1s}	V_{2p}	Mn_{2p}	Cu_{2p}
Raw CAC	76.74	23.26	-	-	-
VO_x/CAC	71.53	28.47	-[a]	-	-
MnO_x/CAC	60.96	29.55	-	9.49	-
CuO_x/CAC	59.33	31.79	-	-	8.87

[a] -: Not detected in XPS examination. However, acid digestion followed by ICP/AES measurements verifies the presence of V on the VO_x/CAC surface.

Table 3. Deconvoluted BE values (eV) and relative areas of components of Mn_{2p}, and Cu_{2p} core excitation obtained from metal oxide-impregnated activated carbons.

Sample	Valance state	Position (eV)	Area (%)
MnO_x/CAC	Mn^{3+}	641.0	18.04
	Mn^{4+}	642.3	81.96
CuO_x/CAC	Cu^{+}	931.8	40.36
	Cu^{2+}	934.1	59.64

Cu^{2+} were the major valence states presenting in the $CuCl_2$-impregnated activated carbon with the corresponding energy at 932.1−932.6 and 934−935.2 eV, respectively (Du *et al*., 2014). Du *et al*. (2014) also showed that after Hg^0 removal test in the simulated flue gas, the spectrum area ratio of Cu^{+} to Cu^{2+} increased from 0.19 to 0.45, which should stem from the oxidation of Cu^{+} by the oxidizing flue gas components. The oxidation of impregnated metal oxides is also expected in our test environment, in which great amounts of O_2 and HCl are present.

In order to understand the crystal forms of metal oxides loading on the activated carbon, XRD analysis was applied to the modified activated carbons. Fig. 3 shows the XRD patterns of the metal oxide-impregnated activated carbons. All the resulting samples had similar XRD patterns, concluding that VO_x, MnO_x, and CuO_x were evenly dispersed on the surface of activated carbon; significant crystalline phases of VO_x, MnO_x, and CuO_x were not present on the surface of activated carbon.

Hg^0 Removal Performance with Activated Carbon under N_2 and Simulation Flue Gas Conditions

The Hg^0 adsorption characteristics and the SO_2/NO removal enhancement for the metal oxide-impregnated activated carbons under N_2 and flue gas conditions are shown in Table 4 and Figs. 4–9. It is noteworthy that all the tests conducted at 150°C did not achieve "equilibrium" during the test time; that is, did not obtain complete breakthrough (i.e., C_o/C_i = 1). Therefore, the Hg^0 adsorption capacities obtained at 150°C shown in Table 4 represent the total adsorption capacities within the 900 min test time, not the actual equilibrium capacities. Table 4 and Figs. 4 and 5 indicate that the Hg^0 adsorption capacity at 150°C increased from 1370.4 to 1698.5 μg g^{-1} under N_2 condition and increased from 1126.6 to 2967.6 μg g^{-1} under flue gas condition after impregnation with metal oxides, respectively. These data indicate that metal oxides-impregnated activated carbons have superior adsorption potential for Hg^0, especially under the flue gas condition for CuO_x/CAC having the greatest Hg^0 removal efficiency of approximately 54.5% at N_2 condition and 98.9% at flue gas condition. The great potentials of using metal oxide-impregnated activated carbons for Hg^0 control are thus demonstrated. Besides the contribution of impregnated metal oxides, acidic and oxidizing components (e.g., O_2, HCl, and NO) coexisting in the flue gas can also greatly enhance the adsorption capacities

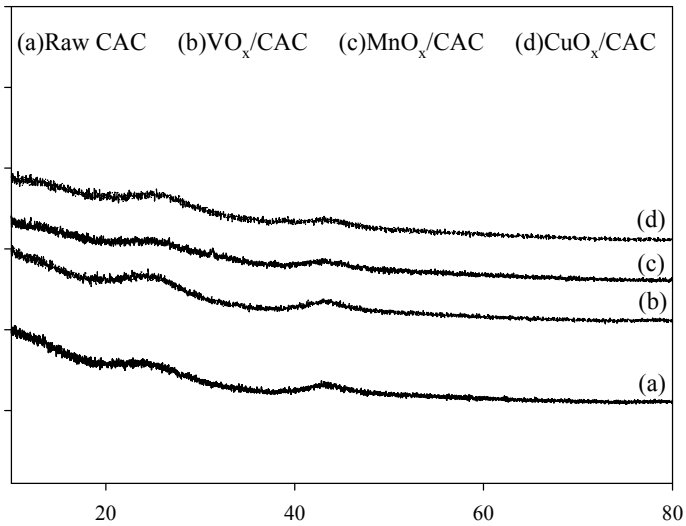

Fig. 3. XRD patterns of raw and metal oxide-impregnated activated carbons.

Table 4. Hg^0, SO_2 and NO removal of raw and transition metal oxide-impregnated activated carbons under N_2 and flue gas conditions

Sample	Ads. time (min)	N_2 condition (150°C)			Flue gas condition (150°C)			N_2 condition (350°C)	Flue gas condition (350°C)		
		C_o/C_i[a]	Ads. capacity ($\mu g\ g^{-1}$)	Avg. Hg^0 removal (%)	C_i/C_o	Ads. capacity ($\mu g\ g^{-1}$)	Avg. Hg^0 removal (%)	Avg. Hg^0 removal (%)	Avg. Hg^0 removal (%)	Avg. η_{SO2} (%)	Avg. η_{NO} (%)
Raw CAC	900	0.81	1370.4	44.8 ± 6.7	0.81	1126.6	35.8 ± 15.1	23.0 ± 3.4	44.8 ± 6.7	1.3 ± 0.9	1.2 ± 0.4
VO_x/CAC	900	0.53	1454.6	48.5 ± 2.2	0.32	2839.0	86.0 ± 6.8	26.1 ± 4.1	48.5 ± 2.2	28.3 ± 3.3	1.9 ± 0.9
MnO_x/CAC	900	0.65	1550.5	50.2 ± 3.3	0.20	2786.3	89.4 ± 5.6	27.7 ± 1.5	50.2 ± 3.3	12.2 ± 2.1	2.0 ± 0.9
CuO_x/CAC	900	0.44	1698.5	54.5 ± 3.6	0.03	2967.6	98.9 ± 0.6	27.1 ± 3.0	54.5 ± 3.6	14.7 ± 1.4	3.7 ± 1.2

[a] C_o/C_i: Hg^0 breakthrough ratio. For here, C_i = Hg Concentration at inlet and C_o = Hg Concentration at outlet.

(Hsi and Chen, 2012). Another study also reported that flue gas components (e.g., SO_2 and H_2O) adversely affected the Hg adsorption because they may interact with the activated carbon surface (Wilcox *et al*., 2012).

It has been well known that Hg^0 control was greatly contributed by oxidation of Hg^0 into Hg^{2+} at elevating temperature, at which the adsorption of Hg becomes thermodynamically unfavorable. Surprisingly, when the temperature increased to 350°C, the metal oxide-impregnated activated carbons still showed 26.1–87.5% Hg^0 adsorption (Table 4 and Figs. 6 and 7), suggesting that strong chemical bonding between Hg and the surface groups of metal oxide-impregnated activated carbons was formed. Among the metal oxide-impregnated activated carbons, the CuO_x/CAC had the greatest Hg^0 control potential at high flue gas temperature. These experimental results are very different with those from other chemically treated activated carbon, such as sulfur-impregnated activated carbon for which the Hg^0 adsorption capacity was completely lost at 350°C. Tian *et al*. (2009) indicated that Hg^0 removal efficiency was around 60% by 3% CeO_2/AC at 30°C. When the temperature increased to 60 and 100°C, the removal efficiency increased to 80% and 85%, respectively. Subsequently increasing the temperature from 100 to 140 and 200°C caused a decrease in removal from 95% to 55% and 27%, respectively. Another study noted that the total adsorbed rate of Hg^0 for $CuCl_2$-impregnated activated carbon was decreased from 90% to 73% when the temperature rose from 60 to 200°C; when the temperature increased to 300°C, the total adsorbed rate was only 6.3% (Du *et al*., 2014). The superior Hg^0 performance of CuO_x/CAC at 350°C is not thoroughly clear at this time, but may stem from its high surface area/microporosity and effective, amorphous, and well distributed Cu functional groups in the activated carbon.

Experimental data presented as steady curves in Figs. 4–7 are imperative, indicating that the Hg^0 removal with metal oxide-impregnated activated carbons was fairly stable and consistent at both 150 and 350°C; significant deactivation in activated carbon did not occur within the 900 min experiment. These results also imply that the metal oxide-impregnated activated carbon may have great potentials to be used as a long-term Hg^0 adsorbent under coal-combustion flue gases and at elevating temperature, which should be further examined in the future.

Enhancement of SO_2/NO Removal for Activated Carbon after Metal Oxide Impregnation

In the study, we also simultaneously investigated the potentials of metal oxide-impregnated activated carbons on enhancing SO_2 and NO removal from the simulated coal-combustion flue gas stream. Table 4 and Fig. 8 show that after metal oxide impregnation, the SO_2 removal by activated carbons was enhanced from 1.3% to > 12% at 350°C. The experimental results also indicated that the VO_x-impregnated activated carbon had the largest SO_2 removal enhancement of approximately 28.3% and the MnO_x-impregnated sample had the lowest SO_2 removal enhancement of approximately 12.2% at 350°C. These experimental data indicate that the active sites for capture

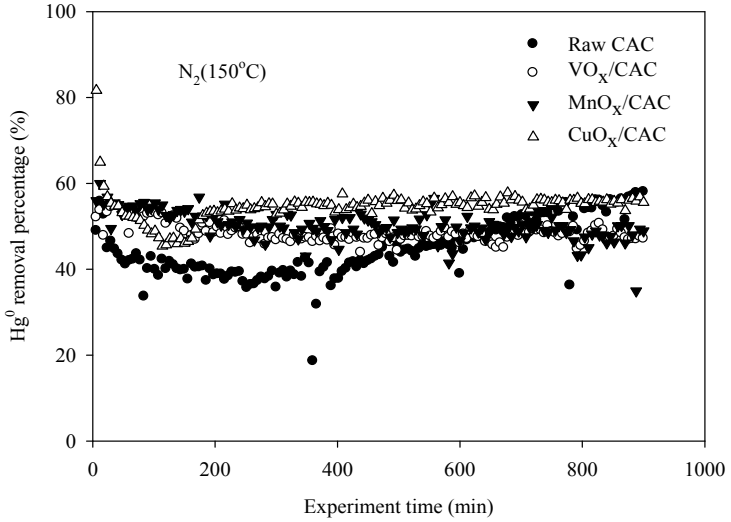

Fig. 4. Hg^0 removal percentage of raw and metal oxide-impregnated activated carbons under N_2 condition (150°C).

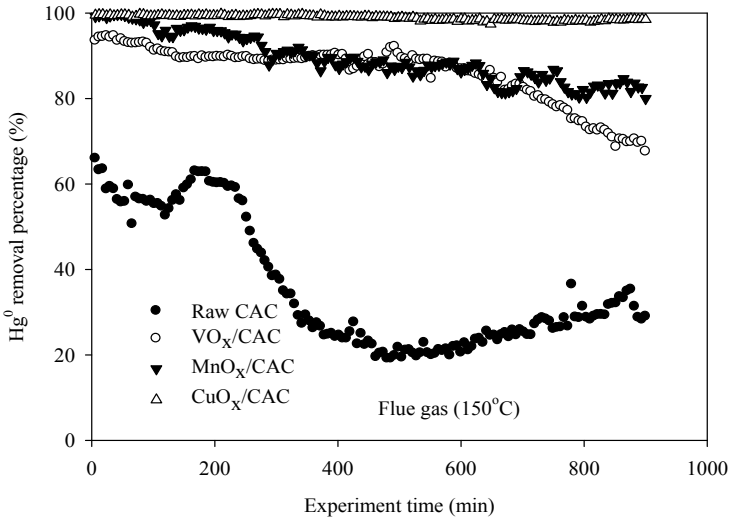

Fig. 5. Hg^0 removal of raw and metal oxide-impregnated activated carbons under flue gas condition (150°C).

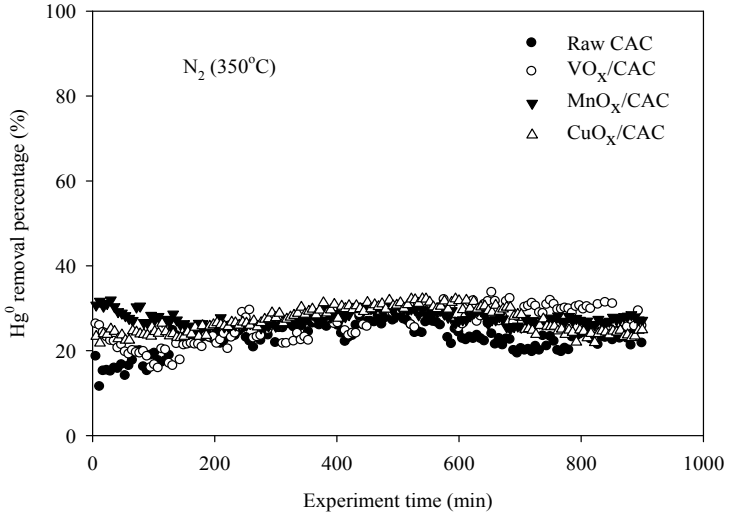

Fig. 6. Hg^0 removal percentage of raw and metal oxide-impregnated activated carbons under N_2 condition (350°C).

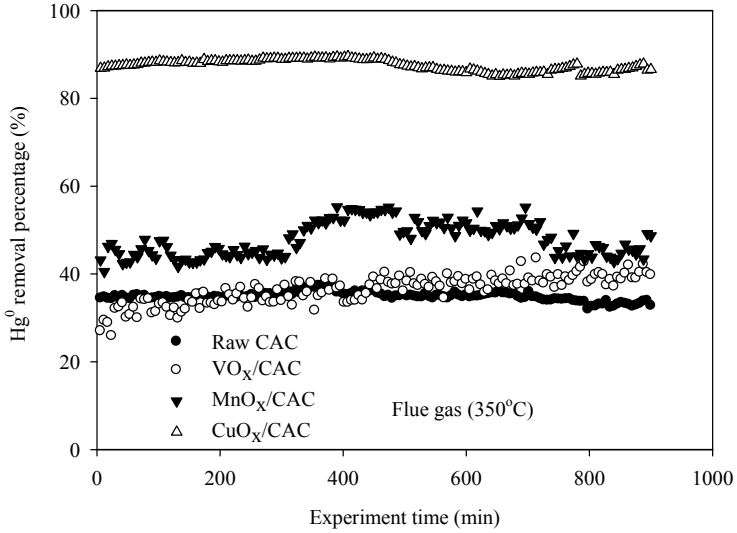

Fig. 7. Hg^0 removal of raw and metal oxide-impregnated activated carbons under flue gas condition (350°C).

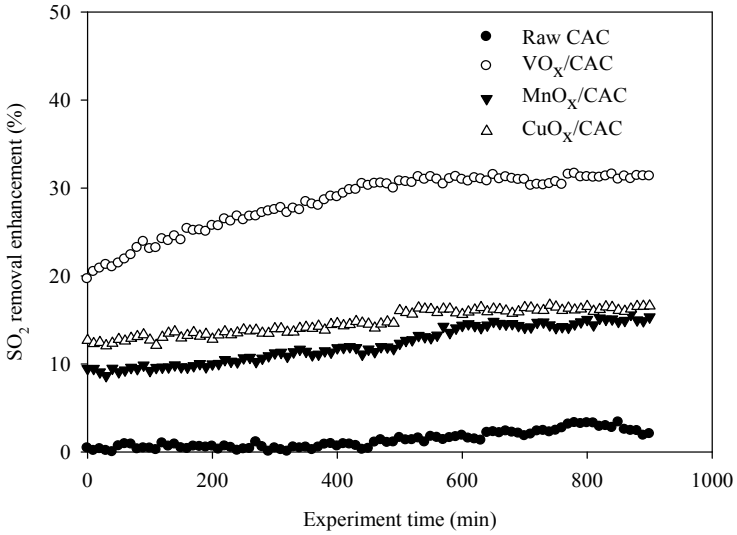

Fig. 8. SO_2 removal enhancement by raw and metal oxide-impregnated activated carbons under simulated coal-combustion flue gas condition (350°C).

or catalytic transformation of SO_2 can be provided by the impregnated transition metal oxides. The larger surface area of the metal oxides-impregnated activated carbons may also lead to more intimate contact with flue gas that either enhance the SO_2–SO_3 conversion and/or direct SO_2 adsorption via the formation of metal sulfate.

Table 4 and Fig. 9 show the NO removal enhancement under the flue gas condition with presence of raw or metal oxide-impregnated activated carbons. After metal oxide impregnation, the NO removal enhancement was slightly improved to 1.9–3.7% at 350°C and the CuO_x/CAC had the largest NO removal. However, the NO removal enhancement of metal oxide-impregnated activated carbons is still very small under flue gas condition, indicating that adsorption of NO may not be a suitable route for NO control; NO reduction on the activated carbon at 350°C also unlikely occurred to enhance NO removal. Consequently, NH_3 may be still needed as a reductant for NO transformation in which metal oxide-impregnated activated carbons are used as reducing catalysts.

CONCLUSION

This study provided understandings on the effects of transition metal oxide (V/Mn/Cu) impregnation on the physicochemical properties and multipollutant Hg^0/SO_2/NO control of a highly microporous activated carbon. After transition metal oxide impregnation, the surface area and pore volume of the sample decreased. SEM images showed that the surface morphology of raw and treated activated carbons was similar after surface modification. The CuO_x/CAC had the greatest Hg^0 removal efficiency at both N_2 and flue gas condition. When the gas temperature elevated to 350°C, the metal oxide-impregnated activated

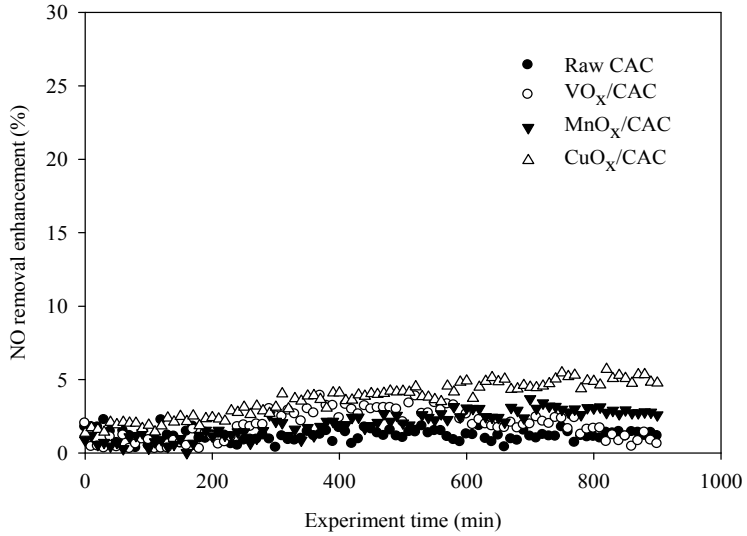

Fig. 9. NO removal enhancement by raw and metal oxide-impregnated activated carbons under simulated coal-combustion flue gas condition (350°C).

carbons still possessed 26.1–87.5% Hg^0 removal. The VO_x-impregnated activated carbon could be used to simultaneously remove Hg^0 and SO_2, but a significant improvement in SO_2 removal enhancement is still needed. The NO removal enhancement of raw and metal oxide-impregnated activated carbons is very small, indicating that adsorption of NO may not be a suitable route for NO control. In the future, injection of NH_3 for catalytic reduction of NO using metal oxide-impregnated activated carbons should be performed to further evaluate the multipollutant removal potential for Hg^0 and NO if the treated activated carbons were considered being used as catalysts.

ACKNOWLEDGEMENTS

Financial support by the Ministry of Science and Technology, Taiwan under Grant no. 100-2221-E-002-256-MY3 is appreciated. We also greatly appreciate the technical assistance from Sheng-Hsuan Hsiao, the Institute of Environmental Engineering and Management, National Taipei University of Technology. The opinions expressed in this paper are not necessarily those of the sponsor.

REFERENCES

Chiu, C.H., Hsi, H.C. and Lin, H.P. (2014a). Multipollutant Control of $Hg/SO_2/NO$ from Coal-Combustion Flue Gases using Transition Metal Oxide-Impregnated SCR Catalysts. *Catal. Today* 245: 2–9.

Chiu, C.H., Hsi, H.C. and Lin, C.C. (2014b). Control of Mercury Emissions from Coal-Combustion Flue Gases Using $CuCl_2$-Modified Zeolite and Evaluating the Cobenefit Effects on SO_2 and NO Removal. *Fuel Process. Technol.* 126: 138–144.

Du, W., Yin, L., Zhuo, Y., Xu, Q., Zhang, L. and Chen, C. (2014). Catalytic Oxidation and Adsorption of Elemental Mercury over $CuCl_2$-Impregnated Sorbents. *Ind. Eng. Chem. Res.* 53: 582−591.

Granite, E.J., Myers, C.R., King, W.P., Stanko, D.C. and Pennline, H.W. (2006). Sorbents for Mercury Capture from Fuel Gas with Application to Gasification Systems. *Ind. Eng. Chem*. Res. 45: 4844–4848.

Hsi, H.C. and Chen, C.T. (2012). Influences of Acidic/ Oxidizing Gases on Elemental Mercury Adsorption Equilibrium and Kinetics of Sulfur-Impregnated Activated Carbon. *Fuel* 98: 229–235.

Hsi, H.C., Rood, M.J., Rostam-Abadi, M. and Chang, Y.M. (2013). Effects of Sulfur, Nitric Acid, and Thermal Treatments on the Properties and Mercury Adsorption of Activated Carbons from Bituminous Coals. *Aerosol Air Qual. Res.* 13: 730–738.

Hu, C., Zhou, J., Li, J., Zheng, J., Wang, Y., Luo, Z. and Cen, K. (2014). Oxidative Adsorption of Elemental Mercury by Activated Carbon from Coconut Shell in Simulated Flue Gas. *Sep. Sci. Technol.* 49: 1062–1066.

Ji, L., Sreekanth, P.M., Smirniotis, P.G., Thiel, S.W. and Pinto, N.G. (2008). Manganese Oxide/Titania Materials for Removal of NO_x and Elemental Mercury from Flue Gas. *Energy Fuels* 22: 2299–2306.

Karatza, D., Lancai, A., Musmarra, D. and Zucchini, C. (2000). Study of Mercury Adsorption and Desorption on Sulfur Impregnated Carbon. *Exp. Therm Fluid Sci.* 21: 150–155.

Li, H., Wu, C.Y., Li, Y. and Zhang, J. (2012). Superior Activity of MnO_x-CeO_2/TiO_2 Catalyst for Catalytic Oxidation of Elemental Mercury at Low Flue Gas Temperatures. *Appl. Catal., B* 111–112: 381–388.

Liu, Q. and Liu, Z. (2013). Carbon Supported Vanadia for Multi-Pollutants Removal from Flue Gas. *Fuel* 108: 149–158.

Li, J.F., Yan, N.Q., Qu, Z., Qiao, S.H., Yang, S.J., Guo, Y.F., Liu, P. and Jia, J.P. (2010). Catalytic Oxidation of Elemental Mercury over the Modified Catalyst Mn/ α-Al_2O_3 at Lower Temperatures. *Environ. Sci. Technol.* 44: 426–431.

Mochida, I., Miyamoto, S., Kuroda, K., Kawano, S.,

Sakanishi, K. and Korai, Y. (1999). Oxidative Fixation of SO_2 into Aqueous H_2SO_4 over a Pitch-Based Active Carbon Fiber above Room Temperature. *Energy Fuels* 13: 374–378.

Mei, Z., Shen, Z., Zhao, Q., Wang, W. and Zhang, Y. (2008). Removal and Recovery of Gas-Phase Element Mercury by Metal Oxide-Loaded Activated Carbon. *J. Hazard. Mater.* 152: 721–729.

Pacyna, E.G., Pacyna, J.M., Sundseth, K., Munthe, J., Kindbom, K., Wilson, S., Steenhuisen, F. and Maxson, P. (2010). Global Emission of Mercury to the Atmosphere from Anthropogenic Sources in 2005 and Projections to 2020. *Atmos. Environ.* 44: 2487–2499.

Stencel, J. and Rubel, A. (1995). Coal-Based Activated Carbons: NO_x and SO_2 Postcombustion Emission Control. *Coal Sci. Technol.* 24: 1791–1794.

Sumathi, S., Bhatia, S., Lee, K.T. and Mohamed, A.R. (2010). Selection of Best Impregnated Palm Shell Activated Carbon (PSAC) for Simultaneous Removal of SO_2 and NO_x. *J. Hazard. Mater.* 176: 1093–1096.

Taiwan Environmental Protection Administration (2013). http://ivy5.epa.gov.tw/enews/fact_Newsdetail.asp?InputTime=1020121160245, Last Access: January, 2015.

Tsuji, K. and Shiraishi, J. (1997). Combined Desulfurization, Denitrification and Reduction of Air Toxics Using Activated Coke: 2. Process Applications and Performance of Activated Coke. *Fuel* 76: 555–60.

Tian, L., Li, C., Li, Q., Zeng, G., Gao, Z., Li, S. and Fan, X. (2009). Removal of Elemental Mercury by Activated Carbon Impregnated with CeO_2. *Fuel* 88: 1687–1691.

Tian, W., Yang, H., Fan, X. and Zhang, X. (2011). Catalytic Reduction of NO_x with NH_3 over Different-Shaped MnO_2 at Low Temperature. *J. Hazard. Mater.* 188: 105–109.

UNEP (2013). UNEP News Centre Website, http://www.unep.org/newscentre/default.aspx?DocumentID=2702&ArticleID=9373&l=zh, Last Access: October 2013.

Wilcox, J., Rupp, E., Ying, S.C., Lim, D.H., Negreira, A.S., Kirchofer, A., Feng, F. and Lee, K. (2012). Mercury Adsorption and Oxidation in Coal Combustion and Gasification Processes. *Int. J. Coal Geol.* 90–91: 4–20.

Yan, N.Q., Liu, S.H., Chang, S.G. and Miller, C. (2005). Method for the Study of Gaseous Oxidants for the Oxidation of Mercury Gas. *Ind. Eng. Chem. Res.* 44: 5567–5574.

Yao, Y., Velpari, V. and Economy, J. (2014). Design of Sulfur Treated Activated Carbon Fibers for Gas Phase Elemental Mercury Removal. *Fuel* 116: 560−565.

Received for review, March 20, 2015
Revised, May 11, 2015
Accepted, July 3, 2015